2013

Exploring the Interplay between Attrition and Separation

Ben J. Freireich
The Dow Chemical Company, USA

Karl V. Jacob
The Dow Chemical Company, USA

EXPLORING THE INTERPLAY BETWEEN ATTRITION AND SEPARATION

Ben J. Freireich[a]* and Karl V. Jacob[a]
[a]The Dow Chemical Company, Core R&D – Solids Processing;
The Dow Chemical Company; Building 1319;
Midland, MI 48640
*T: 1-989-636-3226; F: 1-989-636-4616; E: BJFreireich@dow.com

ABSTRACT
In this work we present a series of progressively more complex models of abrasive attrition and cyclone separation in a circulating fluidized bed (CFB) riser. Regime maps are the presented that illustrate the conditions where the various model complexities are and are not necessary.

INTRODUCTION
It is widely known that higher cyclone inlet velocities produce a finer and tighter gas-particle separation at the cost of higher particle attrition. Determining the optimum cyclone geometry and operating conditions (e.g. inlet velocity and solids loading), therefore, requires consideration of both of these mechanisms. While there exists literature on particle attrition (1, 2) and cyclone collection efficiencies (3, 4), there is a surprising lack of literature on the interplay between both mechanisms.

In general, attrition can be classified into two general categories: abrasion and fragmentation. When particles attrite via abrasion, they continuously shrink in size, usually generating very fine (1-2μm) attrited material. Fragmentation occurs at higher energy and results in a particle breaking into two or more large fragments. In systems that have been designed to limit solids loss, abrasive attrition dominates and fragmentation may be ignored (1, 2). Therefore, in this work, only abrasive attrition is considered.

Within the abrasive attrition literature there are questions as to how particles of varying size attrite. The size dependence of particle attrition has been addressed by several authors (2, 5) resulting in a number of different size dependence models. Intuition suggests that the mass of abraded fines generated is proportional to surface area, implying the rate at which a particle's diameter reduces is independent of particle size. However, empirical data suggest that the rate of diameter reduction can be constant, proportional to particle size (6), or even proportional to the square of particle size (7).

Most studies avoid accounting for collection of attrited fines by assuming that the generated fines have effectively zero size, and are instantly lost from the system (8, 9). On the other hand, Ray et al. (2) have proposed the concept of a *natural particle size* of that fine material. It has been shown that, for many matetrials, regardless of initial particle size or abrasive intensity, the particle size distribution of the attrited fines remains the same (1, 2).

Reppenhagen et al. (10) studied a portion of the problem when they examined the relation between attrition and collection for a cyclone at the end of a

pneumatic conveying line. Here they found, discounting attrition, the cyclone separation efficiency would asymptote towards 100% as inlet velocity was increased. However, when particle attrition was accounted for, a maximum efficiency was achieved. This maximum efficiency was a function of the attritability of the particles. The system studied by Reppenhagen et al. (10) only considered a single pass through the cyclone. In a fluidized bed system, particles will have many passes through the cyclones as they attrite and are eventually lost. The feed particle size distribution, attrition rate, and cyclone collection efficiency will govern the equilibrium particle size distribution (8).

In this work, we examine the combined effects of attrition and cyclone separation at equilibrium conditions by means of a population balance (PB) model. The model will be made progressively more complex by incrementally adding mechanisms so that the influence of each mechanism may be explicitly understood.

THE MODEL

The Model System

The system to be modeled consists of a riser with a close coupled cyclone (**Figure 1**). It is assumed that all of the attrition occurs due to the cyclone, and that all of the material in the bed continuously passes through the cyclone at a rate $\dot{M}$. Close coupling the cyclone avoids the added complexity of bed entrainment as an additional classification mechanism.

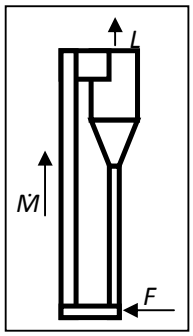

Figure 1: System schematic.

The system is only considered under steady state conditions, such that the solids losses L match the continuous feed rate F. The important dependent variable for this study is the average cyclone collection efficiency $\eta = (\dot{M} - L) / \dot{M}$. The value of η can be computed knowing the particle size distribution (PSD) of particles fed to the cyclone and the cyclone grade efficiency curve $G(x)$ (4). The value $G(x)$ gives the fraction of particles of size x fed to the cyclone that are captured. The relation between G and η is simply $\eta = \int G y dx$, where $y(x)dx$ gives the mass fraction of particles with size between x and $x + dx$.

The Population Balance (PB) Equation

In order to compute the equilibrium particle size distribution we must use a PB

model. A PB model is effectively a mass balance on each differential size class of particles in the system (11, 12, 13). For a derivation similar to that used in this work see Levenspiel et al. (8). We begin by defining the function $m = yM$ where M is the total system mass. The mass balance is written,

$$\frac{\partial m}{\partial t} = \left[\frac{\partial}{\partial x}(Rm) - 3\frac{Rm}{x}\right] - \dot{M}(1-G)\,y + Fy_F \tag{1}$$

The term on the left hand side Eqn. (1) represents the unsteady mass change in a particle size class. The brackets on the right hand side account for mass changes due to attrition. In the brackets, the first term accounts for mother particles leaving size x due to attrition, as well as mother particles that have attrited from the adjacent larger size. The second term within the brackets accounts for mass loss in a size due to fines leaving. Mass that cannot be captured by the cyclone is accounted for by the first term to the right of the bracketed term. Finally, the last term on the right hand side accounts for mass addition.

Integrating Eqn. (1) over all possible sizes results in the macroscopic mass balance equation. Under steady conditions this gives,

$$\eta = \int_{x=0}^{x\to\infty}\left(G - 3\frac{\lambda}{x}\right)y\,dx \tag{2}$$

Here use has been made of the fact that $F = L$ at steady state, and for clarity we have defined the characteristic length $\lambda \equiv MR/\dot{M}$. Physically λ represents twice the thickness attrited during a single pass through the cyclone. Unfortunately, Eqn. (2) is of little use without *a priori* knowledge of the function y. However, we may compute y by solving Eqn. (1). Therefore, at steady state we may eliminate the left hand side and simplify, resulting in the first order non-homogenous linear ordinary differential equation,

$$\frac{dy}{dx} + \left[\left(\frac{d\ln R}{dx} - \frac{3}{x}\right) - \frac{1-G}{\lambda}\right]y = -\frac{1-\eta}{\lambda}\,y_F \tag{3}$$

Equation (3) may be solved for y with an integrating factor. Normalizing y then gives η. In the following sections we will examine the results of Eqn. (3) over a number of different assumptions.

VARIOUS MODELS

Model 0: Using the Feed PSD

The simplest possible approach to the problem is to implement Eqn. (2) directly, setting y equal to the known distribution y_F. This is equivalent to computing the system efficiency for the first instant of time.

For the feed PSD, a log-normal distribution parameterized based on its median x_F and geometric standard deviation σ_g will be used. The cyclone grade efficiency will be described by the empirical grade efficiency from Dirgo and Licht (14),

$$G(x) = \frac{1}{1+\left(\frac{x_{\text{cut}}}{x}\right)^{\beta}} \tag{4}$$

where x_{cut} is the particle size at which 50% of particles are collected, and β

parameterizes the breadth of the grade efficiency function. The efficiency computed by Model 0 is η_0.

Model 1: The Steady State Solution

The next level of complexity employs the PB solution, computing the steady state efficiency from Eqn. (3). Comparison of Model 1 and Model 0 will then give the direct influence of using the steady state distribution vs. the feed distribution. The efficiency computed by Model 1 is η_1.

Model 2: Size Dependent Attrition

Here a level of mechanistic complexity will be added to Model 1 by accounting for a size dependent attrition model. We will employ the general attrition model,

$$R = R_0 \left(\frac{x}{x_0} \right)^n \tag{5}$$

where x_0 is some characteristic particle size (here we will use x_F), R_0 is the attrition rate of that particle size, and n is an exponent defining the size dependence. The efficiency computed by Model 2 is η_2.

Model 3: A Natural PSD

For the last model examined, we will consider the consequences of allowing particles to attrite to a finite size rather than instantly vanishing from the system. Here, we must slightly augment the existing model, because Eqn. (1) was derived assuming vanishing attrited fines.

Finite size fines can be accounted for by simply distributing the mass of fines generated over the natural PSD y_N. Consider that Eqn. (1) was written with every m replaced with m_c, where m_c represents the mass of "coarse" (mother) particles in a differential size class. A similar function m_f represents the mass of attrited fines in a differential size. We then supplement Eqn. (1) with,

$$\frac{\partial m_f}{\partial t} = \left[\int_{x=0}^{x \to \infty} \left(3 \frac{R m_c}{x} \right) dx \right] y_N - \dot{M} (1 - G) y_f \tag{6}$$

where $y_f = m_f/M$. The left most term on the right hand side represents the production of fines distributed over the natural PSD. The right most term is simply the loss of fines from the cyclone. Note, there are no attrition terms in Eqn. (6) because attrited fines do not attrite themselves (2). Under steady conditions we simply have,

$$y_f = \left[\frac{3}{1 - G} \int_{x=0}^{x \to \infty} \left(\frac{\lambda}{x} y_c \right) dx \right] y_N \tag{7}$$

Because Eqn. (3) and Eqn. (7) are only one way coupled they may be solved sequentially. As with Eqn. (3), η is computed by enforcing the normalization condition, $1 = \int (y_c + y_f) dx$. The efficiency computed by Model 3 is η_3.

RESULTS AND DISCUSSION

Model 1

We may interpret the differences between η_0 and η_1 as differences between the feed PSD and the equilibrium bed PSD.
Figure 2 shows a direct comparison between them for typical values of $\sigma_g = 1.4$ and $\beta = 6.0$. For any point on the figure, the grade efficiency curve can be computed using Eqn. (4) and the cut size shown on the abscissa. Both models transition from an attrition dominated regime in the upper left to a separation dominated regime on the lower right. However, Model 1 has a much wider transition region than Model 0. Furthermore, Model 1 predicts lower efficiencies than Model 0 in the attrition dominated regime, while the opposite is true in the separation dominated regime. In the attrition dominated regime, the cut size is so low that particles *must* attrite to be lost by the cyclone. Therefore, in this regime the steady state bed PSD is finer than the feed PSD, causing a higher overall attrition rate (due to a higher specific surface area). In the separation dominated regime, the losses are due mostly to the cyclone's inability to capture mother particles. For this case, the bed PSD is coarser than the feed, because the finest of the feed particles are lost before they have a chance to attrite. A coarser bed PSD then contributes less to attrition losses (due to a lower specific surface area).

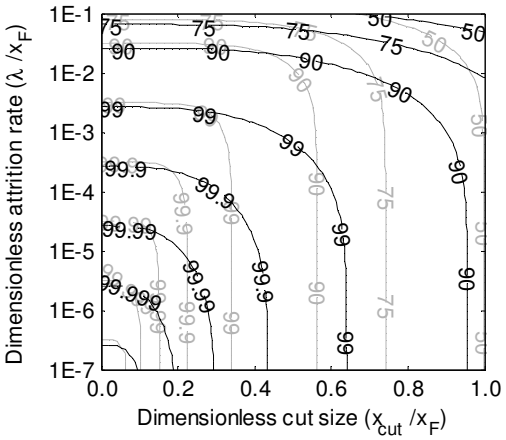

Figure 2: Model 1 and Model 0 results compared. The gray contours represent η_0 while the black contours represent η_1, both for typical values of $\sigma_g = 1.4$ and $\beta = 6.0$. Both efficiencies read in percent.

Model 2

Here we apply size dependent attrition to Model 1. For ease of comparison we adjust λ so that $\lambda \equiv MR_0/\dot{M}$, and set $x_0 = x_F$.
Figure 3 compares Model 2 and Model 1 directly, showing explicitly the consequences of size dependent attrition. In this comparison we have chosen $n = 2$, corresponding to Reppenhagen and Werther (10). It also represents the largest power-law exponent observed in the literature for size dependent attrition, and therefore represents the largest deviation from Model 1.

The discrepancy between Model 2 and Model 1 shown in
Figure 3 is smaller than any of the previous model comparisons made so far in this work. In the attrition dominated regime $\eta_2 > \eta_1$, while the converse is true in

the separation dominated regime. In the attrition dominated regime the steady state bed PSD is slightly finer than the feed PSD, so Eqn. (5) implies that the fines production should be slightly lower. In the separation dominated regime the steady state bed PSD is coarser than the feed, so Eqn. (5) implies the fines production should be slightly higher. For values of $1< n < 2$ the same trend is observed, but less pronounced. Also, for a wider feed PSD the difference between Model 1 and Model 2 is more pronounced, but all of the above results still hold.

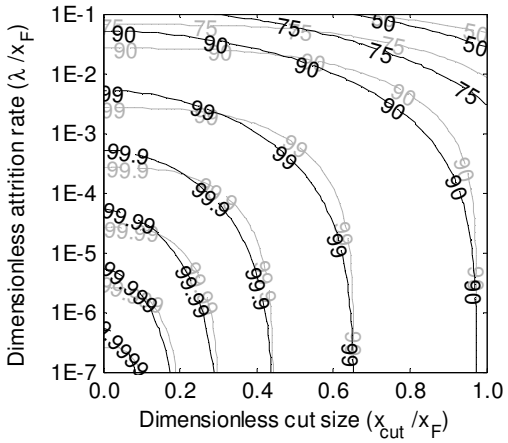

Figure 3: Model 2 (for $n = 2$) and Model 1 results compared. The gray contours represent η_1 while the black contours represent η_2, both for typical values of $\sigma_g = 1.4$ and $\beta = 6.0$. Both efficiencies read in percent.

Model 3

The last of the models to be examined includes non-vanishing fines. A log-normal distribution with, median $0.1x_F$ and geometric standard deviation 1.4, is used for the natural PSD. A comparison of Model 3 to Model 1 is shown in **Figure 4**. For large cut sizes η_3 and η_1 agree almost exactly. When Model 1 is interpreted as applying Model 3 with effectively zero sized fines, this result becomes intuitive. As the cut size shrinks, some of the attrited fines can be captured by the cyclone and the efficiency begins to rise. The steepness of rise of the constant η_3 lines at low cut size is directly related to both the breadth of the natural PSD and the steepness of the cyclone grade efficiency curve (i.e. β).

The difference between Model 3 and Model 1 only arises because the fines in Model 1 are not collectable, while those from Model 3 are. We should, therefore, expect η_3 to always be greater than η_1. This effect can be observed most clearly for the lowest cut sizes, where a significant portion of the natural PSD can be captured by the cyclone. However, we may also observe this effect at higher attrition rates for all cut sizes. In that region the fines are generated faster than the cyclone can remove them.

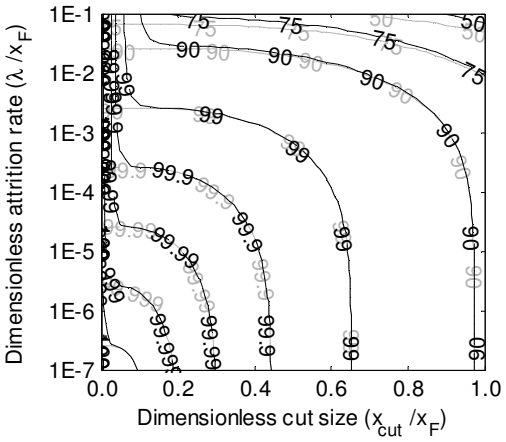

Figure 4: Model 3 (natural PSD with median $0.1x_F$ and $\sigma_g = 1.4$) and Model 1 results compared. The gray contours represent η_1 while the black contours represent η_3, both for typical values of $\sigma_g = 1.4$ and $\beta = 6.0$. Both efficiencies read in percent.

CONCLUDING REMARKS

Plots of cyclone efficiency as a function of attrition rate and cyclone cut size were presented according to four different models: assuming the bed PSD is equal to the feed PSD, assuming size independent attrition and vanishing fines, assuming size dependent attrition, and assuming non-vanishing fines. Comparison of these efficiency maps allows one to determine the influence of each of these mechanisms under their particular operating conditions.

NOTATION

F	Solids feed rate (kg/s)
G	Cyclone grade efficiency (-)
L	Solids loss rate (kg/s)
$\dot{M}$	Solids circulation rate (kg/s)
M	Total system mass (kg)
m	Particle mass distribution (kg/m)
m_c	Mother particle mass distribution (kg/m)
m_f	Attrited fines mass distribution (kg/m)
n	Size dependent attrition power law exponent (-)
R	Abrasion rate (m/s)
R_0	Abrasion rate at characteristic particle size (m/s)
t	Time (s)
x	Particle size (m)
x_0	Characteristic particle size (m)
x_{cut}	Cyclone cut size (m)
x_F	Feed particle median size (m)
y	Particle size distribution (1/m)
y_F	Feed particle size distribution (1/m)
y_f	Attrited fines particle size distribution (1/m)
y_N	Natural particle size distribution (1/m)

β	Cyclone grade efficiency slope (-)
η	Overall cyclone efficiency (-)
η_i	Overall cyclone efficiency compute from model i = 0,1,2,3 (-)
λ	Characteristic attrition length (m)
σ_g	Feed particle size geometric standard deviation (-)

REFERENCES

1. Gwyn, J.E., 1969, "On the particle size distribution function and the attrition of cracking catalysts," *AIChE Journal*, Vol., 15, No. 1, pp. 35-39.
2. Ray, Y.C., Jiang, T.S., and Wen, C.Y., 1987, "Particle attrition phenomena in a fluidized bed," *Powder Technology*, Vol., 49, pp. 193-206.
3. Trefz, M. and Muschelknautz, E., 1993, "Extended cyclone theory for gas flows with high solids concentrations," *Chemical Engineering Technology*, Vol. 16, pg. 153.
4. Hoffman, A.C., and Stein, L.E., 2008, Gas Cyclones and Swirl Tubes, 2nd ed., Springer: New York.
5. Saastamoinen, J.J. and Shimizu, T., 2007, "A model of limestone attrition and SO_2 capture in a large-scale pressurized fluidized bed combustor," *Chemical Engineering Science*, Vol. 62, pp. 574-583.
6. Rangelova, J., Mörl, L., Heinrich, S., and Dalichau, J., 2002, "Decay behavior of particles in a fluidized bed – Application of a mass-related attrition coefficient," *Chemical Engineering Technology*, Vol. 25, No. 6, pp. 639-646.
7. Reppenhagen, J. and Werther, J., 2000, "Catalyst attrition in cyclones," *Powder Technology*, Vol. 113, pp. 55-69.
8. Levenspiel, O., Kunii, D., and Fitzgerald, T., 1968, "The processing of solids of changing size in bubbling fluidized beds," *Powder Technology*, Vol. 2, No. 2, pp. 87-96.
9. Werther, J. and Hartge, E.U., 2004, "Modeling of industrial fluidized-bed reactors," *Industrial Engineering Chemical Research,* Vol. 43, pp. 5593-5604.
10. Reppenhagen, J., Schetzschen, A., and Werther, J., 2000, "Find the optimum cyclone size with respect to fines in pneumatic conveying systems," *Powder Technology*, Vol. 112, pp. 251-255.
11. Hulburt, H.M. and Katz, S., 1964, "Some problems in particle technology: A statistical mechanical formulation," *Chemical Engineering Science*, Vol. 19, No. 8, pp. 555-574.
12. Randolph, A.D. and Larson, M.A., 1971, Theory of Particulate Processes. Academic Press: New York.
13. Ramkrishna, D., 2000, Population Balances: Theory and Applications to Particulate Systems in Engineering. Academic Press: San Diego, 2000.
14. Dirgo, J. and Leith, D., 1985, "Cyclone collection efficiency: Comparison of experimental results with theoretical predictions," *Aerosol Science and Technology*, Vol. 4, No. 4, pp. 401-415.